#3305

BAW-1485
June 1977

69,...

PRESSURE VESSEL FLUENCE ANALYSIS FOR 177-FA REACTORS

By
C. L. Whitmarsh

Prepared for
177 B&W Owners Group
Technical Sub-Committee
for
Reactor Vessel Material
Properties

BABCOCK & WILCOX
Power Generation Group
Nuclear Power Generation Division
P. O. Box 1260
Lynchburg, Virginia 24505

CERTIFICATION

This report has been reviewed for technical content and accuracy.

L. B. Wimmer
Safety Analysis

5 July 1978
Date

Weld composition and location data have been reviewed for accuracy.

Henrik S. Palme
H. S. Palme
Technical Staff

July 11, 1978
Date

Babcock & Wilcox
Power Generation Group
Nuclear Power Generation Division
Lynchburg, Virginia

Report BAW-1485

June 1979

Pressure Vessel Fluence Analysis for 177-FA Reactors

C. L. Whitmarsh

Key Words: Neutron Fluence Measurement, Neutron Fluence Prediction, Neutron Dosimetry, Pressure Vessel Surveillance, Neutron Transport, Pressurized Water Reactor, Discrete-Ordinates Analysis, Surveillance Capsules

ABSTRACT

A necessary part of a surveillance program required to monitor pressure vessel physical properties is an analytical method of predicting fast flux distribution in the pressure vessel. In addition, there is a need to predict fluence (and therefore flux) over the vessel's design life, which necessitates flux extrapolation over multiple fuel cycles. An analytical model was developed based on two-dimensional transport theory. The reference model is in planar geometry with appropriate correction factors for capsule perturbation effects and axial power distribution. An important feature of the model is the inclusion of a point-by-point relative power distribution which has been averaged over the irradiation time period. Integral flux comparisons with dosimeter data from five operating reactors indicated agreement of fast flux ($E > 1$ MeV) within 15% based on fission reactions in ^{237}Np and ^{238}U. Uncertainty limits for calculated fast flux were estimated to be ±20% at the inside surface of the pressure vessel and ±30% for that value extrapolated to 32 EFPY. Based on this analytical procedure, a generic design curve is presented for predicting the pressure vessel fluence expected in a 177-FA reactor over its 32 EFPY design life.

CONTENTS

List of Tables

List of Figures

1. INTRODUCTION

The reactor vessel surveillance program (RVSP) was established to monitor the combined effects of irradiation and temperature on the mechanical properties of the beltline region materials in a reactor. The RVSP became a requirement in the early 1960's when it was determined that significant differences occurred in the neutron embrittlement sensitivity between various steels and weldments used in reactor construction. These regulations are published in Appendixes G and H of 10 CFR 50.[1,2] Of major importance is the adjustment of the reference nil ductility temperature (RT_{NDT}) as a function of fast neutron fluence (E > 1 MeV). This information will affect operating limitations with respect to normal heatup and cooldown procedures for the reactor vessel. These pressure-temperature limits are part of the Technical Specifications imposed on the operating license required for each reactor.

The initial program, which was designed for Oconee-class reactors, consisted of four holder tubes located in the coolant inlet region between the thermal shield and the pressure vessel.[3] Each holder tube contained two capsules filled with specimens of pressure vessel materials similar to those used in vessel fabrication. Also contained in each capsule were dosimeters for monitoring flux exposure. During first-cycle operation, mechanical problems with holder tubes were encountered in several reactors, which necessitated the removal of surveillance capsules from all reactors in the original program. The affected plants are Arkansas Nuclear One, Unit 1; Three Mile Island Nuclear Station Unit 1, Rancho Seco Nuclear Generating Station Unit 1, and Oconee Nuclear Station Units 1, 2, and 3. These specimens, and others, were then added to the RVSP (with redesigned holder tubes) in three reactors scheduled for later startup — Three Mile Island Nuclear Station Unit 2, Crystal River Unit 3 Nuclear Generating Plant, and Davis-Besse Nuclear Power Station Unit 1. Because reactors were now operating without surveillance capsules, an analytical determination of fluence was required; i.e., fluence accumulation by the reactor vessel in one reactor had to be correlated with the fluence of test

specimens irradiated in another reactor. In addition, prediction of future fluence exposure is necessary for component design and for establishing withdrawal schedules for surveillance capsules.

Prior to the RVSP a generic fluence value was calculated using the analytical procedure available at that time and published in BAW-10100A.* Because of uncertainties in reactor operating conditions and the lack of applicable experimental data to benchmark the analytical procedure, considerable conservatism was incorporated into this curve. When surveillance capsules were removed from five of the six operating 177-FA reactors, fluence data became available for comparison. This provided an opportunity to reduce conservatism in the design curve by better defining reactor operating conditions and refining the analytical flux calculations on which fluence is based. This report describes that effort.

By their very nature, generic design curves will be conservative for most reactors because they represent the most adverse conditions expected to occur in a class of reactors. Also, the fluence curve refers to the spatial location in the pressure vessel at which the integrated flux (over vessel life) will be a maximum. This curve is based on a fluence calculation using cycle 1 reactor conditions that has been extrapolated to equilibrium cycle reactor conditions. Thus, the two primary concerns are (1) the ability to calculate fluence for a known set of conditions and (2) the ability to extrapolate that fluence to conditions existing in an equilibrium cycle. An additional problem is the predictability of reactor conditions associated with an equilibrium cycle (defined as the reactor cycle that will predominate over the vessel lifetime of 32 effective full power years -- EFPY). An evaluation of these uncertainties will be included in this report.

2. ANALYTICAL MODEL

2.1. Important Variables

The analytical determination of fast flux (E > 1 MeV) that reaches the reactor pressure vessel can be considered as two basic problems: (1) calculation of the fast flux that escapes the core and (2) attenuation of that flux from the core to the pressure vessel. Determination of fluence adds an additional complication — the flux must be time-averaged over the irradiation period to provide a value that, when multiplied by time, will produce fluence.

For a given relative power density (RPD) distribution and core configuration, fast flux that escapes the core is directly proportional to reactor power level. Also, for a given reactor core configuration, fuel loading, and power level, the flux that escapes the core is a function of RPD distribution represented in three dimensions. RPD distribution, in turn, is a function of fuel enrichment, lumped burnable poison (LBP), and control rod locations. In B&W reactors a zoned core design is utilized wherein one third of the fuel assemblies are replaced by fresh assemblies at the end of each fuel cycle. Thus, enrichment distribution (and therefore RPD distribution) varies from one cycle to the next due to fuel management procedures. In addition, LBP and fissionable material burnup and control rod movement cause the RPD to vary during a fuel cycle. Consequently, a detailed description of reactor operating conditions is required in order to calculate an RPD representative of an irradiation period. RPD is utilized in the particle transport codes DOT and ANISN as a fixed source (fission density) input which has been normalized to reactor power level. Because of this dependence on reactor operating conditions, RPD distribution (and therefore flux escaping the core) can vary from one reactor to another. However, differences are expected to be small because of similar operational conditions.

For a given relative flux spectrum, attenuation of flux between the core and the pressure vessel is primarily a function of the configuration of reactor internal components, their materials of construction and the coolant density.

Since relative flux spectrum at the core edge is determined by the core configuration and fuel type, all 177-FA reactors have essentially the same spectrum exiting the reactor core. In addition, all 177-FA reactors have the same nominal configuration of internal components and materials and operate with nearly the same coolant temperatures. Thus, flux attenuation from core edge to pressure vessel should be about the same for all 177-FA plants. Small differences may result from the possibility of cross mixing of fluxes in the X-Y plane (plan view through the core). This results from RPD variation in the azimuthal (θ) direction (peripherally around the core) as well as in the radial (R) and axial (Z) directions.

Obviously, an accurate calculation of this attenuation is difficult considering the approximations required to simulate real geometry in a computer code. However, if the attenuation calculation for a typical RPD distribution has been benchmarked and isolated from other effects, the problem of calculating pressure vessel fluence would be primarily that of calculating fast flux escaping from the reactor core.

2.3. Initial Generic Model Improvement

A generic design curve for fast fluence at the reactor pressure vessel, published in BAW-10100A[4], was based on information and methods available in early 1975. Considerable conservatism was intentionally included in this model because of uncertainties in reactor operating conditions and the absence of any comparative experimental data. The calculational model consisted of one-dimensional geometry, which was then corrected to the peak axial and azimuthal flux location using separately calculated factors. The transport code ANISN[5], which solves the Boltzmann transport code using the method of discrete ordinates, was used to calculate a multigroup radial flux distribution from the core through the pressure vessel. The model included a radial RPD distribution for an estimated equilibrium cycle, coolant water at 600F, and a 10% safety factor.

Specific items of concern were the assumptions that radial and azimuthal effects were independent, the 600F coolant temperature was too high, and the estimations of RPDs. The availability of dosimetry data from cycle 1 surveillance capsules led to the use of a two-dimensional, R-θ geometry model using more realistic coolant temperatures and RPDs. A detailed description of this model is included in section 2.3. This updated model permitted a reduction in the built-in conservatism.

Although not directly related to the generic design curve, another calculation is required to define the beltline region. This requires a two-dimensional model in R-Z geometry. The initial model[4] contained most of the conservatisms and deficiencies that existed in the generic curve calculation.

2.3. Calculational Model

2.3.1. Configuration

A major effort in analytical modeling is the simulation of actual three-dimensional (3-D) shapes by using one- (1-D) and two-dimensional (2-D) code geometries. Multi-dimensional treatment and geometric detail are severely limited by available computer storage. In addition, material properties should be representative of average conditions during the irradiation period. Although inlet coolant temperature does increase at power levels below full power (~2.5°F per 10% power change), the total time at a fractional power level relative to the length of an irradiation period is usually small, and this effect can be ignored. Thus, approximations and trade-offs are required and are selected in such a way as to minimize any effect on final results.

The ANISN[5] and DOT[6] particle transport codes were used for 1-D and 2-D calculations. Both codes use the discrete ordinates method of solution of the Boltzmann transport equation and have multi-group and asymmetric scattering capability. The reference calculational model is an R-θ geometric representation of a plan view through the reactor core midplane and includes core, core liner, coolant, core barrel, thermal shield, and pressure vessel. One-eighth core symmetry is used based on structural configuration and RPD data (Figure 2-1 and Table 2-1). Code parameters were limited to P_3 order of scattering, S_8 quadrature, and 22 energy groups in order to include reasonable geometric detail. Flux generation in the core was represented by ^{235}U fission distribution, which the code derives from the input RPD and a normalization factor to adjust flux level to the desired power density. Reflected upper and lower boundary conditions are used to represent core and structural symmetry. The right boundary (outside surface of pressure vessel) requires an albedo boundary condition to simulate flux leakage across that boundary and to adequately describe the perturbation caused by the concrete primary shield. Energy-dependent albedos were calculated from a 1-D model using the ANISN code in cylindrical geometry with major axis dimensions and RPD distribution, and including the pressure vessel cavity and primary concrete shield regions.

For those reference calculations that did not require accurate fluxes near the edge of the pressure vessel, the right albedo could be replaced by a vacuum condition that tended to simplify calculational effort.

The P_1 order of scattering does not adequately describe the predominately forward scattering of neutrons observed in deep penetration of steel and water media. This necessitated calculation of a P_3/P_1 correction factor using a P_3, S_6, 22-group, 1-D cylindrical model in ANISN with major axis dimensions and RPD. Reference model correction factors were determined by calculating the ratio of fast flux (E > 1 MeV) from the 1-D model to the 2-D model. These values were obtained as a function of radial location along the major axis (Table 2-2). Since these factors are primarily dependent on geometry and materials between the core and the capsule location, the values should be applicable to all 177-FA reactors, and no significant dependence on azimuthal (θ) location is expected.

The S_6 symmetric quadrature has generally produced accurate results in discrete ordinates solutions for similar problems. No significant change in fluxes was attained with the use of S_8 quadrature. No further verification of quadrature accuracy was made.

The 22-group neutron microscopic cross sections represent the neutron portion of a shielding-oriented, coupled, 40-group set, DLC-23/CASK.[7] With this set the fast neutron energy range (E > 1 MeV) is represented by the first 11 groups plus a portion of group 12 (Table 2-3). Macroscopic cross sections, required for transport analyses, were then obtained with the mixing code TAFMAKE[5]. Nominal compositions were used for the structural metals. Coolant compositions were determined from the average boron concentration over a fuel cycle and the bulk temperature of the region. The core region was a homogeneous mixture of fuel, fuel pins, structure, and coolant.

2.3.2. Relative Power Density Distribution

For a given power level the neutron flux escaping the reactor core boundary is directly related to the RPD distribution in the core, e.g, as RPD values are increased near the core periphery, the flux increases proportionately. RPD distributions in three dimensions must be considered. During a fuel cycle, fuel burnup and control rod movement tend to cause the RPD to vary; between fuel cycles the movement of fuel assemblies causes variations. For the

surveillance model it is convenient to obtain a time-averaged RPD so that an average flux can be calculated to represent this transient behavior over an irradiation period. Thus, fluence can be obtained from the product of the average flux and the time interval over which it applies.

Pin-by-pin RPDs are generated in criticality and fuel management analyses which have been demonstrated to be accurate predictions of actual RPDs in operating reactors.[8] Thus, RPD values at 1.44-cm intervals (pin pitch) are obtained for Mark B fuel assemblies. These data are utilized in the surveillance program as input to transport codes where RPD values are internally converted to fission densities and, as such, represent a flux source in the calculation model. Because the mean free path (mfp) for fast neutrons in the core region is 10 to 30 cm, only neutrons born in the outer two rows of assemblies significantly contribute to flux escaping the core. Thus, particular detail is required near the core periphery.

RPD data are generated at about 8 to 12 points in time during a fuel cycle so that the transient behavior can be approximated with static calculations. For transport model input, these data are time-averaged to produce a single RPD that will represent the entire irradiation period of interest. The averaging method assumes linear RPD variation with time except when control rods are moved, and then a step change occurs. An example of this method is presented in Appendix A. Conversion of RPD data from the XY spatial mesh used in criticality analyses to that used in the surveillance reference model (R.) requires the use of the subsidiary code SORREL[9].

The analytical procedure for a reference model calculation is to use the XY (or RΘ) RPD data (time-averaged) for a specific reactor irradiation period for which dosimetry data are available and then adjust the results (section 2.3.5) to equilibrium cycle conditions to obtain generic fluence results. RPD data in XY geometry are available for all reactor fuel cycles for which the cycle time and enrichment distribution have been predetermined. Because of the fuel shuffle pattern generally followed — one third of the fuel assemblies are replaced by fresh fuel after each fuel cycle — the third and succeeding fuel cycles should be similar and are referred to as equilibrium cycles.

Since the reference model calculation produces fluxes in only the X and Y dimensions, an axial correction factor (F_z) is required to adjust these

values to the axial location (Z dimension) of interest. The XY RPD data are all evaluated at an average axial location $(q/\bar{q})_z = 1.0$. The axial RPD distribution is primarily a function of control rod movement and is considered to be independent of the XY (or RΘ) data. An average axial correction factor is evaluated for the axial location of interest that represents the axial shape of flux at the core edge (Appendix B). That shape is assumed to apply throughout the RΘ calculation model, i.e., flux values at all RΘ locations use the same axial correction factor. Calculated axial factors for each reactor analyzed to date are listed in Table 2-4.

When 1-D model calculations (ANISN) are performed, the input RPD distribution is obtained from the corresponding XY or (RΘ) data by using the values along a major axis only. Thus, ANISN-calculated fluxes should correspond to those along a major axis in a DOT RΘ model.

2.3.3. Beltline Region

Closely associated with the generic curve calculation is the definition of the beltline region in a reactor. For this purpose a 2-D RZ calculational model is needed to obtain the required isofluence lines. Azimuthal dependence (Θ dimension) is eliminated by correcting calculated fluxes to the Θ location with maximum flux. The methodology for the calculational model is essentially the same as that described in section 2.3.1 except for geometry. Radial boundaries, which represent cylindrical surfaces in RZ geometry, relate to dimensions along a major axis. The cavity and the primary concrete shield regions external to the pressure vessel are included to account for axial flux streaming. Because of computer storage limitations, two calculational models are necessary — upper half of the core plus related internal structure and lower half of the core plus structure. Figure 2-2 is a schematic of an upper core model; a similar model is used for the lower reactor region. Input RPD distribution is formulated from the product of the 1-D radial RPD (major axis) and an estimated equilibrium cycle axial RPD[10]. Both RPD distributions are time-averaged over an equilibrium fuel cycle.

Calculated flux along the midplane of the RZ model is normalized to the RΘ reference model after allowance for the relative axial power at that location. This flux distribution is then converted to fluence (multiplication by time) and plotted as limiting isofluence values for various concentrations of phosphorus and copper.*

2.3.4. Capsule Model

The presence of a surveillance capsule in a reactor perturbs the flux measured by the dosimeters. Therefore, comparison of experimental to calculated flux requires that this effect be determined. Since the capsule was not included in the R0 reference model because of computer storage limitations, it was necessary to obtain a correction factor that could be applied to reference model data. Thus, a capsule perturbation factor, J(E), was calculated to represent the relative flux change (as a function of energy) that would occur if the capsule were included in the reference model.

A 2-D calculational model (P$_3$S$_8$ 28-group) was formulated in XY geometry to explicitly represent the surveillance capsule (Figure 2-3). Although exact geometry could not be represented in the XY coordinate system, boundaries were followed reasonably well, and cross sectional areas of capsule materials were equated to real areas. A source was input into a 1-cm-thick core barrel region that reproduced the same relative flux energy spectrum at the outer edge of the thermal shield region that existed in a R0 reference model calculation. This procedure was necessitated by code limitations (no provision for angular flux input). Inclusion of a separation distance from the thermal shield outer surface to the core barrel was required to generate the appropriate angular flux from the isotropic source input. Several iterations were required to create the correct spectrum; the output spectrum from one calculation was used to adjust the source input to a succeeding calculation. The capsule cross section in Figure 2-3 is representative of the Charpy specimen region (Figure 2-4). Any flux differences that might be caused by using a tensile specimen region were considered small.

Two calculations were made — one with the Figure 2-3 configuration and one with water substituted for the capsule materials. The ratio of the average flux in the specimen region from the two calculations was defined as J(E). Factors were calculated for energy ranges consistent with dosimeter reactions and reported fluxes of interest (Table 2-5). A factor greater than one indicates that the capsule materials do not remove (by downscattering and absorption) as many neutrons as an equivalent water region. The symmetric location of dosimeters at the outer edge of the specimen region led to the use of specimen region average flux as the calculation criterion. To verify this selection,

factors were also calculated using the average flux in the Al filler region and results were essentially the same.

Comparison of dosimeter measurements to calculated fluxes requires that a reference location be selected. The dosimeters were symmetrically located with respect to the center of the capsule (plan view). Thus, an average of the four dosimeter measurements should correspond to the average flux in the specimen region. Point (or mesh interval) values are more conveniently obtained from code calculations. Data from the capsule model calculation indicated that the flux value located at the center of the capsule was the same as the specimen region average value. Therefore, all comparisons of measured to calculated data will be based on values calculated at the location of the capsule center.

2.3.5. Fluence Extrapolation

The prediction of fluence for future fuel cycles with known power distributions (fuel distributions and burnups) is of primary concern. In a 177-FA reactor the transport of fast neutron flux from the core edge to the pressure vessel is solely dependent on relative spectrum at the core edge, structural component geometry, and materials of construction. Since all 177-FA plants are quite similar in these respects, the ratio of fast flux at the pressure vessel (ϕ_{pv}) to fast flux that escapes the core (ϕ_{ce}) should be constant. Thus, the following procedure is proposed for predicting pressure vessel flux (and therefore fluence) prior to performing a complete analysis.

Spatially averaged PDQ fast flux (E > 1.85 eV) in the core liner is a quantity readily available from criticality calculations, which are included in the fuel management analyses required for all operating plants. These data are considered to be proportional to the fast flux which escapes the core and ultimately reaches the pressure vessel. Values from each time step are weighted in order to obtain a time averaged flux that can be used to calculate fluence. These values were observed to increase up to 20% from beginning- to end-of-cycle depending on control rod manipulation. Pressure vessel time-averaged flux can then be predicted by

$$\phi_{pv}(A) = \frac{\phi_{ce}(A)}{\phi_{ce}(B)} \times \phi_{pv}(B)$$

where A and B represent fluence periods which are generally defined for a specific reactor and a specific fuel cycle.

Since our interest is in fluence (or flux) at the maximum location, azimuthal flux variations are important. However, implicit in this procedure (use of spatially averaged flux) is the assumption that significant variations in azimuthal flux peaking do not occur between fuel cycles. To date, sufficient experience has not been obtained to evaluate this assumption although indications are that it is correct.

Available flux data are listed in Table 2-6 for 177-FA reactor plants which are presently operating without surveillance capsules. Comparison of predicted-to-normalized values from a surveillance capsule analysis indicates good agreement. However, capsule data are sparse and, in general, represent similar conditions (cycle 1 conditions) A more rigorous comparison using cycle 2 and 3 results is considered necessary to verify this procedure for extrapolating fluxes from one reactor cycle to another. However, the procedure does have a good theoretical basis and comparisons to reference model calculations for ANO-1, cycles 3 and 6 show good agreement.

For comparative purposes, pressure vessel maximum flux (cycle averaged) has been calculated for all reactor cycles for which PDQ analyses are available (Table 2-6). Note the similarity between reactors for assumed equilibrium cycles (cycle 3 and later). Fluxes for SMUD are somewhat higher primarily because of its higher power level (2772 MWt). ANO-1 (cycles 4, 5, and 6) is a special case because Arkansas Power & Light has recently made a decision to use an 18-month LBP fuel cycle. Other utilities are contemplating such a move but none is definite as yet.

2.4. Future Improvements

The analysis procedure described herein was developed during the course of analyzing the initial group of surveillance capsules. Since analytical model development is a continuing process, a number of areas where techniques could be improved have been noted.

Of the items under consideration, major emphasis should be given to the use of the code DOT IV, an improved version of DOT. Improved data storage, restart capabilities, convergence, and variability of quadrature and dimensions should permit P_3 scattering detail and explicit capsule geometry to be

incorporated into the reference model. This would eliminate the need for those correction factors used in the present method.

Other improvements, judged to have lesser individual significance are:

1. Use of component dimensions that exist at reactor operating conditions as opposed to "cold" dimensions.
2. Calculation of axial flux shape that exists at the capsule and pressure vessel locations as opposed to using the relative power distribution in peripheral fuel assemblies.
3. Determination of the flux distribution within a capsule to better define specific dosimeter and/or specimen exposure.
4. Correction of dosimeter measurements for attenuation of flux through dosimeter tube and wire holder wall thicknesses.
5. Refinement of spectral shape used for flux weighting of dosimeter capture cross sections.

Table 2-1. Reference Calculation Model

Component	Material	Outer radial dimension along major axis, cm
Core	Homogenized mixture of UO_2 fuel, Zr-4 cladding, H_2O coolant, and Inconel structure	163.79
Core liner	SS 304	165.697
Bypass coolant	H_2O (500 ppm B) @ 580°F and 2200 psi	179.37
Core barrel	SS 304	184.15
Inlet coolant[a]	H_2O (500 ppm B) @ 555°F and 2200 psi	186.69
Thermal shield	SS 304	191.77
Inlet coolant[a]	H_2O (500 ppm B) @ 555°F and 2200 psi	216.694
Pressure vessel[b]	A508 Class 2 steel	238.444

[a] Full power condition.

[b] SS 304 vessel cladding is included as an integral part of the pressure vessel, minimum thickness = 0.317 cm.

Table 2-2. P_3/P_1 Order of Scattering Correction to Reference Model Calculations

Energy range, MeV	Capsule location	Pressure vessel wall
>0.1	1.22	1.29
>0.5	1.23	—
>1.0	1.23	1.29
>2.3	1.25	—
>2.5	1.25	—

Table 2-3. Energy Structure of Cross Section Set

Group	Upper energy, MeV	Energy width, MeV	Lethargy width	Average[a] energy, MeV
1	15	2.8	0.20	13.5
2	12.2	2.2	0.20	11.1
3	10	1.82	0.20	9.05
4	8.18	1.82	0.25	7.19
5	6.36	1.40	0.25	5.60
6	4.96	0.90	0.20	4.49
7	4.06	1.05	0.30	3.50
8	3.01	0.55	0.20	2.73
9	2.46	0.11	0.05	2.42
10	2.35	0.52	0.25	2.08
11	1.83	0.72	0.50	1.42
12	1.11	0.56	0.70	0.78
13	0.55	0.439	1.60	0.25
14	0.111	0.107	3.50	1.93(-2)
15	3.35(-3)[b]	2.77(-3)	1.75	1.41(-3)
16	5.83(-4)	4.82(-4)	1.75	2.44(-4)
17	1.01(-4)	7.2(-5)	1.25	5.45(-5)
18	2.9(-5)	1.83(-5)	1.00	1.76(-5)
19	1.07(-5)	7.64(-6)	1.25	5.74(-6)
20	3.06(-6)	1.94(-6)	1.00	1.86(-6)
21	1.12(-6)	7.06(-7)	1.00	6.83(-7)
22	4.14(-7)	4.14(-7)	—	—

[a] Based on 1/E flux variation over the energy group.

[b] Read as 3.35×10^{-3}.

Table 2-4. Axial Correction Factor to Reference Model Calculation

Reactor	Cycle	Axial correction factor: Capsule location[a]	Axial correction factor: Pressure vessel wall[b]
Oconee 1	1	1.1[c]	1.1[c]
	2	1.1[c]	1.1[c]
Oconee 2	1	1.14	1.17
Oconee 3	1	1.17	1.18
TMI-1	1	1.1[c]	1.1[c]
ANO-1	1	1.17	1.13

(a) Averaged over capsule length for that portion of cycle while capsule was in reactor.

(b) Maximum value.

(c) Estimated.

Table 2-5. Surveillance Capsule Flux Perturbation Factors

Energy range, MeV[a]	Dosimeter reaction	J(E)	
>0.1	—	1.90	1.33
>0.5	$^{237}Np(n,f)^{137}Cs$	1.81	1.26
>1.0	$^{238}U(n,f)^{137}Cs$	1.71	1.19
>2.3	$^{58}Fe(n,p)^{58}Co$	1.46	1.03
>2.5	$^{54}Fe(n,p)^{54}Mn$	1.45	0.99

(a) See Appendix C for determination of effective energy range for dosimeter reactions.

Table 2-6. Data for Pressure Vessel Fluence Prediction in 177-FA Reactors

Reactor	Fuel cycle	Spatial and time averaged flux ($E > 1.85$ eV) in core liner, ϕ_{ce}	Flux at pressure vessel surface, ϕ_{pv} ($E > 1$ MeV)	
			Value from ϕ_{ce} ratio[a]	Normalized value from capsule analysis
Oconee 1	1	—	—	1.37(10)
	2	7.05(13)[d]	2.03(10)	2.08(10)
	4	5.81(13)	1.68(10)	—
Oconee 2	1	4.82(13)	Ref.	1.39(10)
	2	5.60(13)	1.61(10)	—
	3	6.13(13)	1.77(10)	—
	4	6.13(13)	1.77(10)	—
Oconee 3	1	4.73(13)[b]	1.36(10)	1.39(10)
	2	5.68(13)	1.64(10)	—
	3	6.21(13)	1.79(10)	—
TMI-1	1	4.82(13)	1.39(10)	1.45(10)
	2	5.48(13)	1.58(10)	—
	3	5.60(13)	1.61(10)	—
	4	5.93(13)	1.71(10)	—
ANO-1	3	6.20(13)	1.79(10)	1.74(10)[c]
	4 (LBP)	3.96(13)	1.14(10)	—
	5 (LBP)	4.45(13)	1.28(10)	—
	6 (LBP)	4.37(13)	1.26(10)	1.32(10)[c]
SMUD	2	6.89(13)	1.99(10)	—
	3	6.56(13)	1.89(10)	—

[a] Uses Oconee 2, cycle 1, as reference value.

[b] Partial cycle prior to removal of surveillance capsule.

[c] Direct calculation using reference analytical model and capsule normalization factor from cycle 1 analyses.

[d] Read as 7.05×10^{13}.

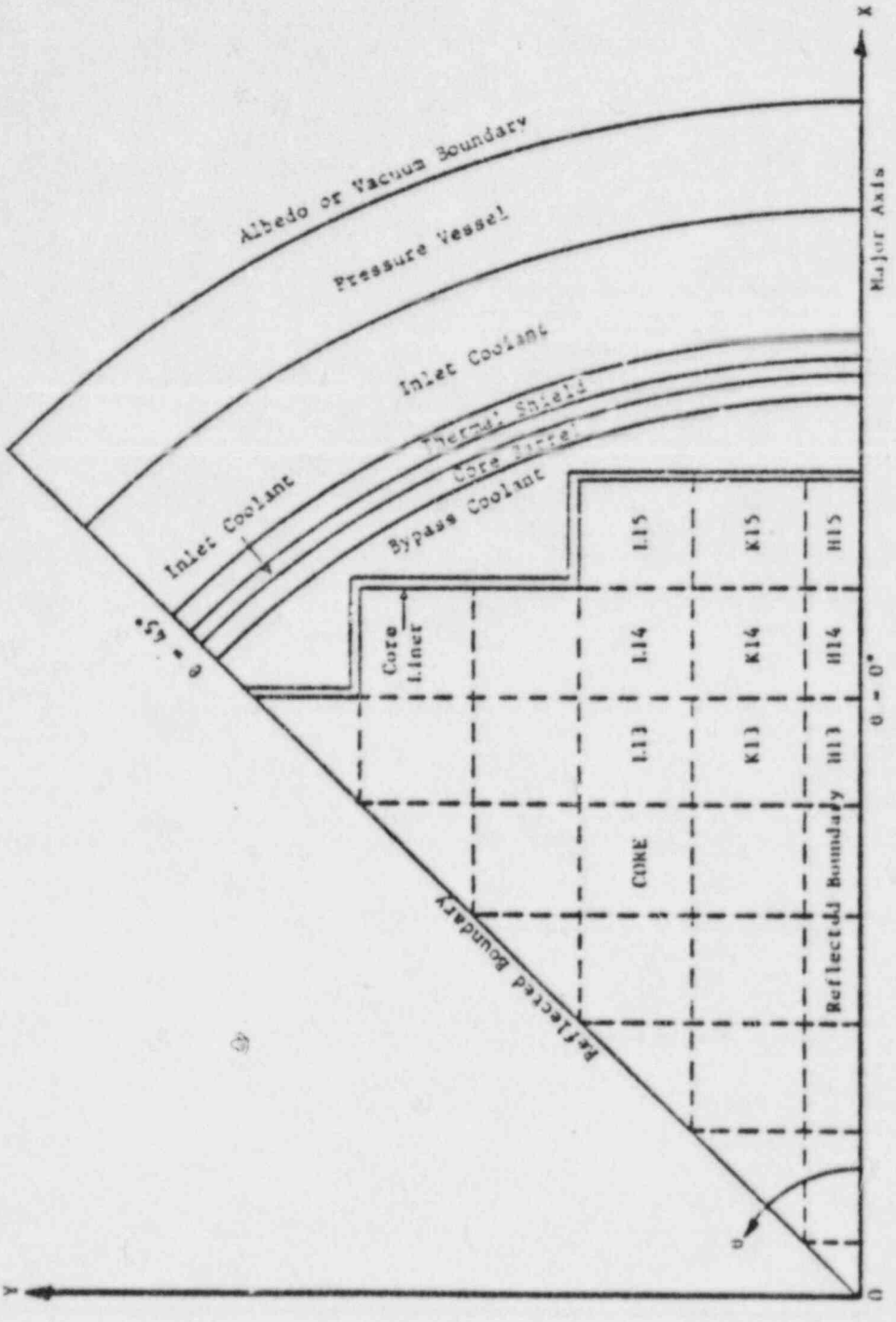

Figure 2-1. Plan View Through Reactor Core Midplane (Reference R-θ Calculation Model)

Figure 2-2. Cylindrical Model of Upper Reactor Internals (Beltline Region Calculational Model)

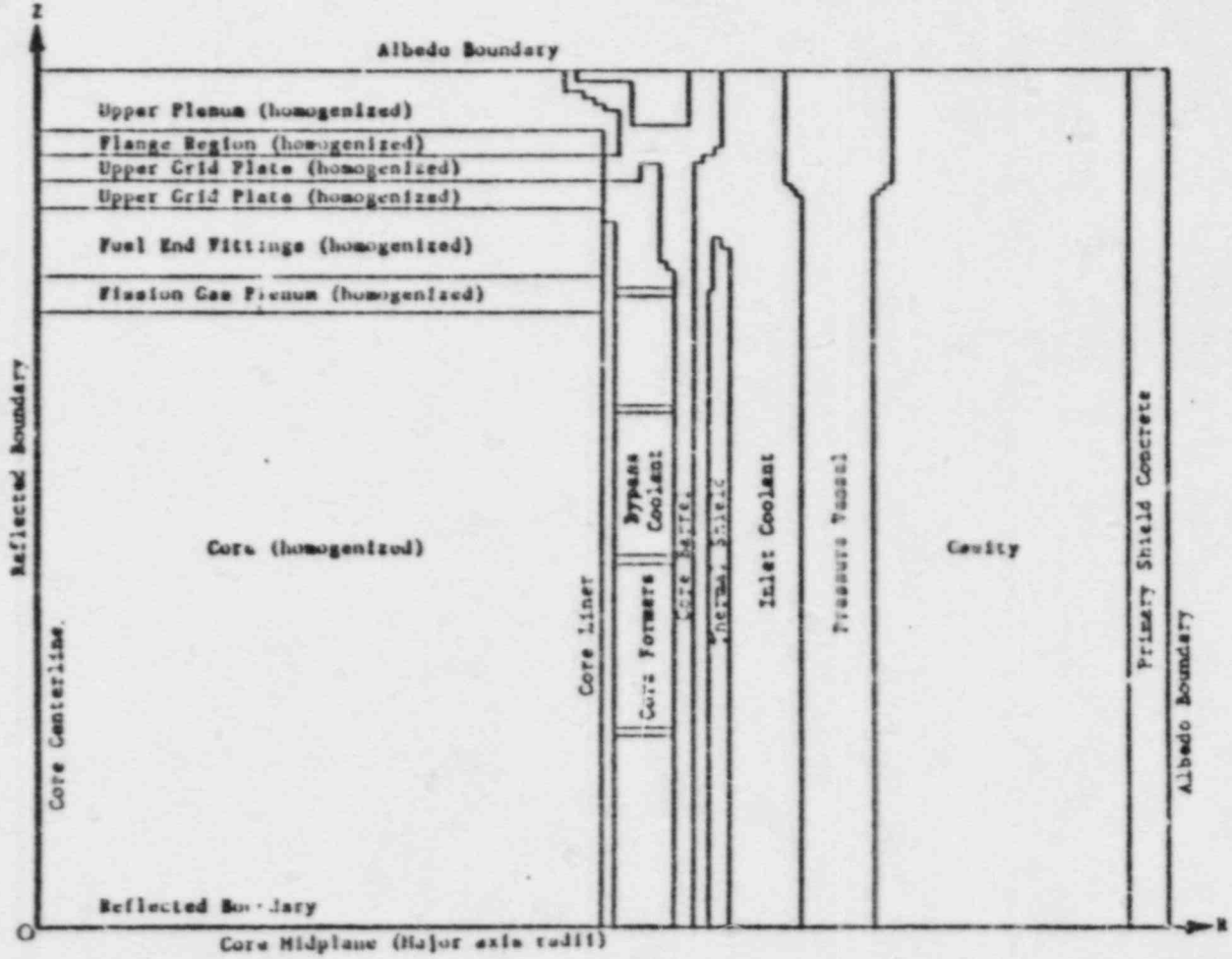

Figure 2-3. Geometric Model for Calculation of Capsule Perturbation Effect on Flux

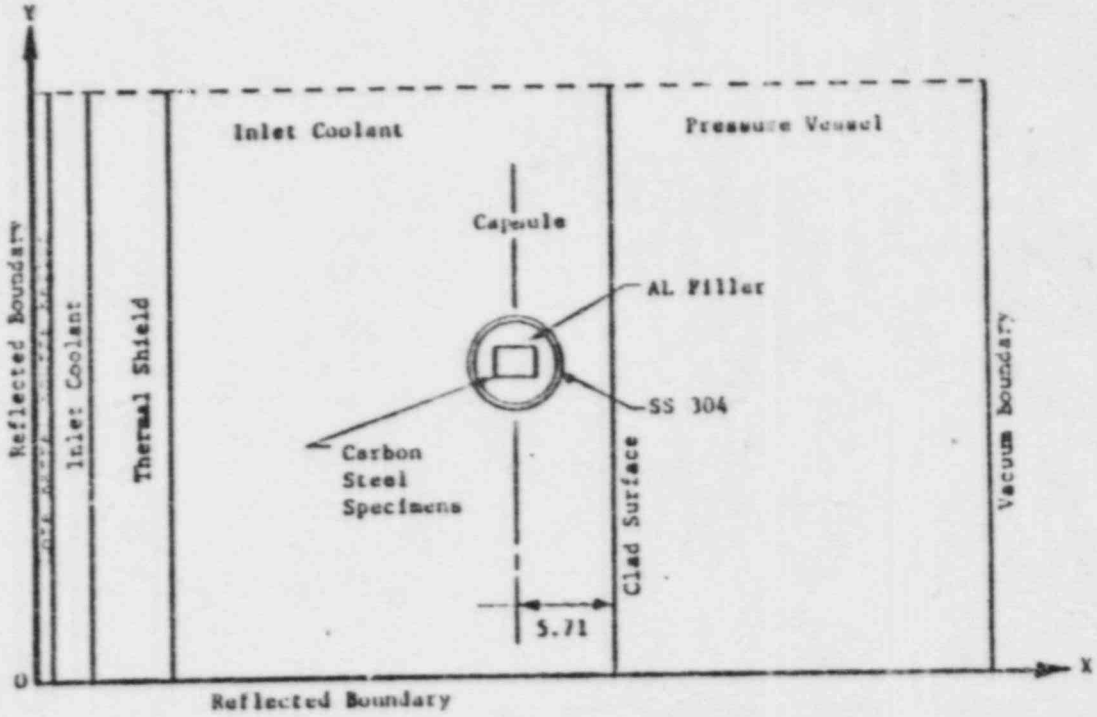

Figure 2-4. Surveillance Capsule Arrangement

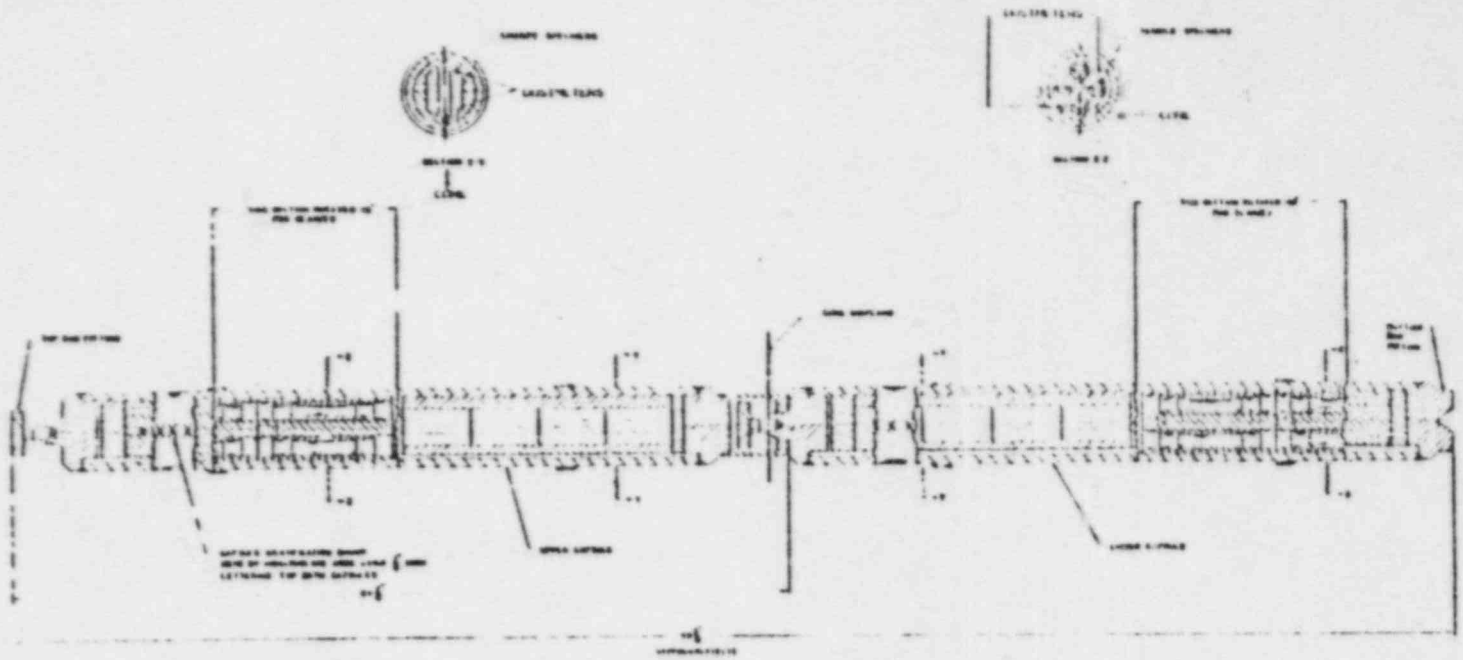

BLANK FRAME

FOR

PROPER PAGINATION

3. EXPERIMENTAL BASIS

3.1. Dosimeters

Dosimetry for long term fast fluence measurements requires that the target material have a significant capture cross section over the appropriate energy range. This is necessary so that sufficient reactions occur with neutrons in the energy range of interest. In addition, a reaction product with a long half-life is desirable, preferably on the order of the irradiation period or greater. This insures that the dosimeter activity is a record of reactions that have occurred over the entire irradiation period. If short-lived products were utilized, reactions that occur early in the irradiation period would decay to the point that the measured activity would represent only the flux that existed during the latter part of the time period. Obviously, for a constant flux irradiation, product half-life would not affect the analysis; but that condition rarely exists in commercial reactor operation.

For pressure vessel surveillance, dosimeter reactions of interest are listed in Table 3-1. However, only the fission reactions in ^{237}Np and ^{238}U satisfy both energy and longevity requirements. The ^{58}Ni and ^{54}Fe dosimeters are useful for supporting data with appropriate adjustment for energy range and time-averaged flux. The ^{59}Co dosimeters are used to estimate total and thermal flux. The target materials are ~40 mil diameter wires of high purity materials which are contained individually in holder tubes of Al or Cd-Ag alloy. These holder tubes are assembled end-to-end in a dosimeter tube (Figure 3-1). Four identical dosimeter tubes are contained in each surveillance capsule (section 2.3.4). Because of their symmetrical location relative to the specimens, average data were considered representative of the interior region of the capsule. Also, the elevation differences (two dosimeter tubes in the upper section and two in the lower section) were considered insignificant because of the relatively flat axial flux shape at the capsule elevation. As part of the integrated surveillance program, capsules and dosimeters are being redesigned to provide additional target materials for better spectral analysis and redundancy.

3.2. Dosimeter Activation

3.2.1. Measurement Procedure

After a prescribed irradiation period, capsules were removed from a reactor and transported to the Lynchburg Research Center (LRC) for disassembly. Dosimeter wires were manually removed and then counted with a Ge-Li detector connected to a multi-channel analyzer. Target material weights were obtained from wire weights and associated chemical and isotopic compositions. Measured activities were reported as μCi/g of target material.

Because wire dosimeters are flux accumulators, no distinction is made with respect to the energy of the incident flux or to the rate-history of exposure. Thus, a significant analytical effort is required to define spectral shape of the flux and its magnitude as a function of time.

3.2.2. Analytical Procedure

To provide a basis for comparison of measured-to-analytical data, calculated flux was converted to activity. This is accomplished with the following equation.

$$D = \frac{Nf}{(3.7 \times 10^{4})M} \sum_{E} \sigma(E)\phi(E) \sum_{j} F_j \left\{ 1 - e^{-\lambda_i t_j} \right\} e^{-\lambda_i (T - \tau_j)}$$

where

- D = dosimeter activity, μCi/g of target material n,
- f = fission yield of target material n (= 1 for non-fission materials),
- N = Avagadro's number,
- M = atomic weight of target material n, grams,
- $\sigma(E)$ = group averaged microscopic activation cross section for material n, barns/atom,
- $\phi(E) = K(E)\phi(E)$ = neutron flux obtained from reference model calculation with appropriate correction factors, n/cm²-s,
- $K(E)$ = combined flux correction factor = $P_j/P_i \times F_g \times J(E)$,
- $\phi(E)$ = neutron flux from reference model calculation, n/cm²-s,
- F_j = fraction of reactor full power during j^{th} time interval,
- λ_i = decay constant for isotope i, s^{-1},
- t_j = time interval for irradiation period j, s.

T = total calendar time from reactor startup to shutdown for capsule removal, s,

τ_j = time interval from reactor startup to end of j^{th} irradiation period, s.

For each reactor the flux integral, $\int_E \sigma(E)\phi(E)$, was calculated in the reference model as $\int_E \sigma(E)\cdot(E)$ and then multiplied by the appropriate correction factors as follows:

$$K(E) \int_E \sigma(E)\phi(E) = \int_E \sigma(E)K(E)\phi(E) = \int_E \sigma(E)\phi(E).$$

The activation cross section $\sigma(E)$, were obtained by flux weighting ENDF/BIV data over a fission spectrum for the required group structure (see Appendix D). Although initial weighting was based on a fission spectrum in lieu of knowledge of the actual spectrum "seen" by the dosimeters, a later comparison of calculated spectra was made (Table 3-2). The net effect on dosimeter activity of cross section over the various spectra, although not determined quantitatively, was considered small based on a similar unreported comparison. Of course, there is no guarantee that the calculated spectra are correct even though the calculation techniques are considered theoretically correct. Experimental spectrum determination was not feasible because of the previously noted lack of long-lived dosimeter reactions available.

The power integral, $\int_j F_j \left\{ 1-e^{-\lambda_i t_j} \right\} e^{-\lambda_i (T-\tau_j)}$ is a measure of isotope decay prior to reactor shutdown. (No allowance was made for subsequent decay because measured data were reported for zero time after shutdown). Fractional power traces, obtained from on-line instrumentation, were input to an auxiliary computer code for each isotope of interest. Thus, a power integral was generated for each isotope over each reactor history. Implicit in this procedure is the assumption that relative power density does not vary with power level.

3.1.3. Comparison of Data

In order to benchmark calculated fluxes and to verify the analytical procedure used to determine flux distribution and spectra, measured dosimeter activities were compared to calculated activities. Implicit in this procedure is the assumption that measured-to-calculated activity ratios are equivalent to flux ratios. This can be shown to be true if the calculated flux spectrum is

identical to the actual spectrum seen by the dosimeter (see Appendix E). On this basis the surveillance capsule dosimetry data were correlated. (These data have previously been published for each capsule analysis in references 11 through 16).

Because of their effective energy range and long half-life product, the $^{237}Np(n,f)^{137}Cs$ and $^{238}U(n,f)^{137}Cs$ reactions were considered to best represent fast flux to the surveillance capsules averaged over the irradiation period. The corresponding normalization factors (measured-to-calculated flux ratio) are listed in Table 3-3 for each reactor. The data fall within a narrow band of 0.99 to 1.17, which suggests that calculated flux may be somewhat low. However, it should be noted that all are within the uncertainty band (see section 4) although a bias does occur. Considering the many variables in the analytical procedure, the comparison is quite good and is considered to be a verification of the analytical procedure for calculating fluxes in the capsule. By inference, calculated fluxes in the pressure vessel should have about the same accuracy. For conservatism, a normalization factor of 1.1 was selected to apply to all calculated fluxes.

Ancillary dosimetry data are listed in Table 3-4 which generally support the observations above. However, both the $^{54}Fe(n,p)^{54}Mn$ and $^{58}Ni(n,p)^{58}Co$ reactions were shown to have normalization factors consistently less than 1.0 (overprediction of flux by calculational procedure). Although no explanation presently exists for this phenonenon, it is suspected that the calculated flux spectrum is overpredicted in the energy range greater than ~4 MeV. If such a condition does exist, any effect on $^{237}Np(n,f)$ and $^{238}U(n,f)$ reactions would be much less, ~2% and 7% respectively, because relatively more of those reactions occur at lower energy. Any effect on integrated fast flux (or fluence) would be similarly diminished because of the relatively small fraction of flux with energy greater than ~4 MeV. Consequently, the importance of these data are discounted with respect to normalization of calculated fast flux. However, the above discussion does illustrate the danger of directly applying dosimetry data to other energy ranges. Should the specimen evaluation procedure be altered in the future to include an energy dependent damage analysis, spectral shape of the flux will become more important and such suspected discrepancies should be reconciled. In addition, the importance of Oconee 1 data was discounted because of undefined problems that occurred in the measurement of cycle 1 dosimeters.

Some verification for the prediction of flux similarity between 177-FA reactors (section 2.1) for similar irradiation periods (fuel cycles) is obtained by comparing activity measurements with the power integral divided out. This removes the effects of reactor operating history and length of the irradiation period from the activity. Thus, a significant variation in measured activity was reduced to an almost constant value (Table 3-5) which indicates that the fast flux was essentially the same in each reactor. The variation in power integral values is indicative of different operating histories and irradiation times. Calculated fast flux was also essentially constant between reactors. Analytical models differed only in the input power distributions which were similar for cycle 1 in each reactor.

Table J-1. Dosimeter Reactions

Target material[a]	Reaction	Product	Half-life[b]	Effective energy range, MeV[c]
^{237}Np[d]	n,f	^{137}Cs[e]	30.03 y	>0.5
^{238}U[f]	n,f	^{137}Cs[e]	30.03 y	>1.1
^{58}Ni[g]	n,p	^{58}Co	71.23 d	>2.3
^{54}Fe[h]	n,p	^{54}Mn	312.6 d	>2.5
^{59}Co[i]	n,γ	^{60}Co	5.266 y	total
^{59}Co[i]	n,γ	^{60}Co	5.266 y	>0.3 eV

[a] All materials except ^{54}Fe and one of the ^{59}Co are contained in Cd-Ag holder tubes to eliminate thermal neutron flux.

[b] See reference 17.

[c] See Appendix C.

[d] 1.44 weight % Np, 100% isotopic.

[e] Although all fission products are produced, ^{137}Cs is of primary importance because of its high yield and long half-life.

[f] 10.38 weight % U, 99.27% isotopic.

[g] 100 weight % Ni, 67.77% isotopic.

[h] 100 weight % Fe, 5.82% isotopic.

[i] 0.56 weight % Co, 100% isotopic.

Table 3-2. Comparison of Relative Flux Spectra

Group	Lower energy bound, MeV	Fission	Spectra Normalized to E > 1 MeV			
			In H_2O at capsule location	Capsule center	Pressure vessel Wall	Pressure vessel T/4
1	12.2	0.0002	0.0016	0.0013	0.0015	0.0013
2	10	0.0013	0.0064	0.0054	0.0064	0.0053
3	8.19	0.0052	0.018	0.015	0.018	0.014
4	6.36	0.021	0.050	0.041	0.047	0.035
5	4.96	0.031	0.092	0.074	0.081	0.060
6	4.06	0.052	0.078	0.063	0.069	0.049
7	3.01	0.159	0.118	0.098	0.099	0.076
8	2.46	0.132	0.122	0.109	0.106	0.092
9	2.35	0.034	0.039	0.037	0.034	0.031
10	1.63	0.178	0.152	0.162	0.153	0.133
11	1.11	0.323	0.278	0.334	0.320	0.382
12[a]	1.0	0.044	0.046	0.060	0.066	0.099

[a] Partial group.

Table 3-3. Normalization Factors for Calculated Flux in Surveillance Capsules

Reactor	Cycle	Dosimeter reaction	Dosimeter activity, dps/g Measured	Dosimeter activity, dps/g Calculated	Normalization factor[a]
Oconee 1	1	$^{237}Np(n,f)^{137}Cs$	(b)	3.19	--
		$^{238}U(n,f)^{137}Cs$	(b)	0.64	--
Oconee 1	1,2	$^{237}Np(n,f)^{137}Cs$	9.32	8.80	1.06
		$^{238}U(n,f)^{137}Cs$	1.94	1.72	1.13
Oconee 2	1	$^{237}Np(n,f)^{137}Cs$	6.70	5.81	1.15
		$^{238}U(n,f)^{137}Cs$	1.21	1.22	0.99
Oconee 3	1	$^{237}Np(n,f)^{137}Cs$	5.42	4.65	1.17
		$^{238}U(n,f)^{137}Cs$	1.05	0.98	1.12
TMI-1	1	$^{237}Np(n,f)^{137}Cs$	7.33	6.40	1.15
		$^{238}U(n,f)^{137}Cs$	1.42	1.24	1.15
ANO-1	1	$^{237}Np(n,f)^{137}Cs$	5.20	4.39	1.17
		$^{238}U(n,f)^{137}Cs$	0.97	0.93	1.04

(a) Normalization factor = measured activity/calculated activity.

(b) Measured values were inconsistent with similar data and, therefore, were considered to be incorrect.

Table 3-4. Ancillary Dosimetry Data

Reactor	Cycle	Normalization factor, measured activity/calculated activity					
		$^{54}Fe(n,p)^{54}Mn$	$^{58}Ni(n,p)^{58}Co$	$^{237}Np(n,f)^{103}Ru$	$^{238}U(n,f)^{103}Ru$	$^{237}Np(nf)^{95}Zr$	$^{238}U(n,f)^{95}Zr$
Oconee 1	1	0.76	1.07	--	--	--	--
Oconee 1	1,2	0.74	0.77	1.06	0.99	--	--
Oconee 2	1	0.86	0.90	1.13	1.02	1.20	1.04
Oconee 3	1	0.85	0.91	1.23	1.12	1.27	1.11
TMI 1	1	0.83	0.96	1.18	1.29	--	--
ANO-1	1	0.98	0.91	--	1.15	--	--

Table 3-5. Activity and Flux Comparison Between Reactors

Reactor	Cycle	Measured[a] activity, μCi/g	Power integral	K × FI,[b] μCi/g	Calculated[c] flux in capsule, n/cm²-s
Oconee 2	1	6.70	0.0268	250	2.48(10)
Oconee 3	1	6.42	0.0214	253	2.48(10)
TMI-1	1	7.23	0.0293	247	2.62(10)
ANO-1	1	5.20	0.0204	255	2.44(10)

[a] Average of four dosimeters for $^{237}Np(n,f)^{137}Cs$.

[b] K × FI = measured activity/power integral.

$$K = \frac{fN}{(3.7 \times 10^{4})M},$$

FI = flux integral = $\int_g \sigma(E)\phi(E)$.

[c] Average value for E > 1 MeV.

Figure 3-1. Surveillance Capsule Dosimeters

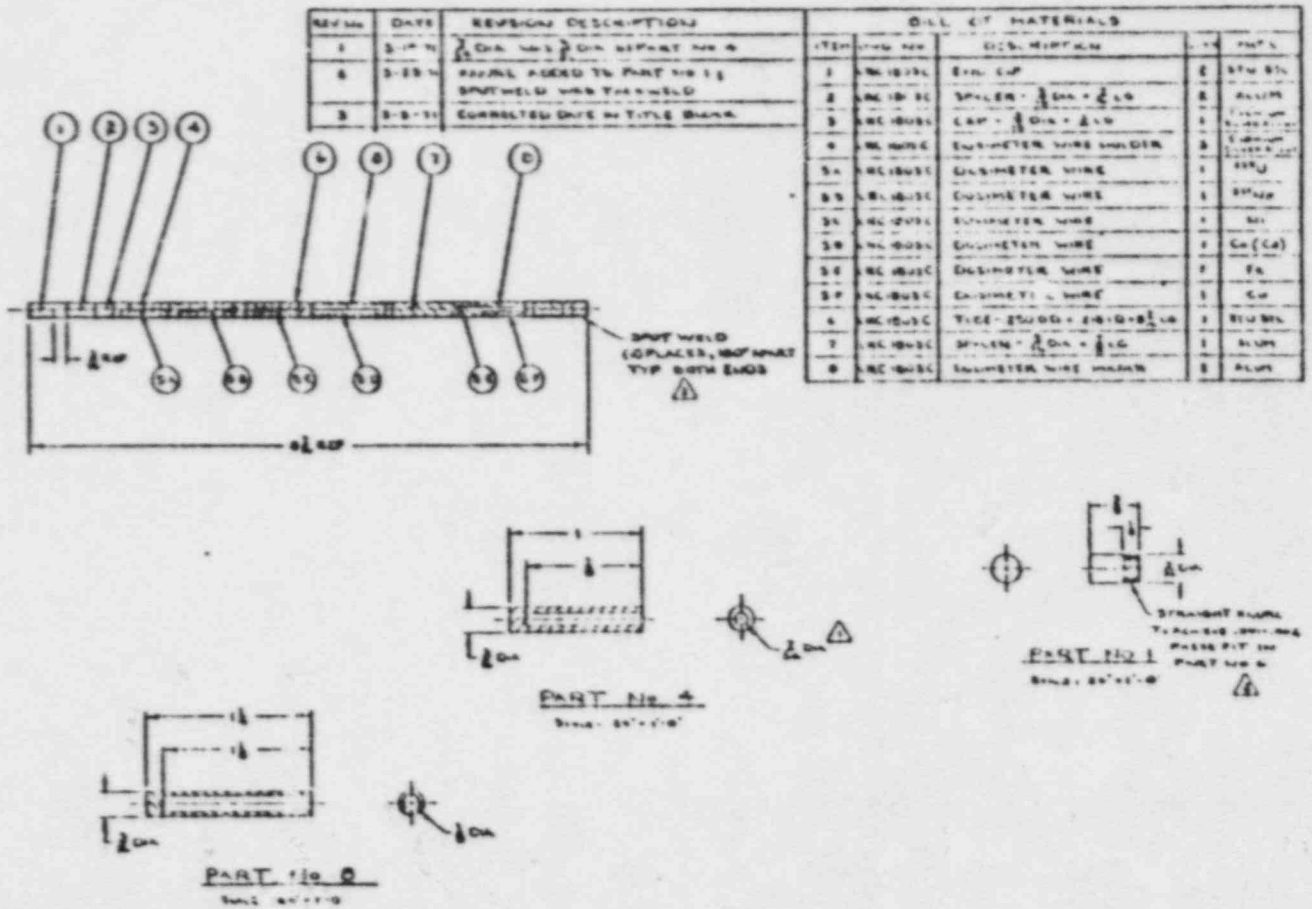

Babcock & Wilcox

BLANK FRAME

FOR

PROPER PAGINATION

4. ANALYSIS OF DATA UNCERTAINTY

Flux values determined in the surveillance program are subject to uncertainties related to dosimeter activation measurements, calculated conversion of activity to flux, and prediction methods for extending data to future reactor operation. A recent study was performed at B&W to define uncertainty limits for measured and calculated flux data[18] and those results are summarized in this section.

4.1. Surveillance Capsule Analysis

Ranges of data uncertainties for the various phases of this analysis are listed in Table 4-1. Limit values for measured activities were calculated in reference 18 and include components for dosimeter wire weighing, composition of target material in the wire, gamma counting statistics, instrumentation calibration, and possible misalignment of the capsule holder tube in a reactor. Major contributors to the overall uncertainty limits were calibration and positioning errors. Detector calibration was ±7% and the capsule position was assumed to be within ±0.25 inches of its designated location. Limit values for the $^{237}Np(n,f)$ reaction exceeded other reaction data due to greater uncertainty of the composition of ^{237}Np in the dosimeter wire.

Evaluation of uncertainty limits related to calculated activities includes consideration of such components as approximations in the transport theory model, microscopic neutron cross sections, material compositions, three-dimensional relative power distributions, capsule model geometric approximations, fission yields, averaging of neutron cross sections over energy groups for dosimeter reactions, isotope decay constants, and measurement of reactor power history. Because of their interdependent and sometimes complex effects on activity, limits for most of these components were necessarily estimated based on experience and engineering judgment.

Conversion of measured activity to flux requires the use of neutron cross sections for dosimeter reactions, fission yields, and knowledge of reactor power

history during the irradiation period. Implicit in this analysis is the assumption that relative power distribution is independent of power level. Inclusion of limits for these components causes the uncertainty limits of the measured activities to increase (Table 4-1). For some reactions an extrapolation is required to extend measured flux to the fast flux energy range (>1 MeV). Possible errors in spectral shape were estimated to have a ±10% effect on total fast flux. This additional uncertainty tends to decrease confidence in $^{54}Fe(n,p)$ and $^{58}Ni(n,p)$ reaction measurements for fast flux calculations relative to the two fission dosimeters.

4.2. Generic Flux Data

Since calculated activities for the initial group of surveillance capsules (Tables 3-3 and 3-4) were essentially all within uncertainty limits for measured activities, it would seem reasonable to conclude that the analytical procedure has been verified. (A 1.1 factor was applied to calculated fluxes to account for an apparent negative bias and to insure conservative results). Consequently, uncertainty limits associated with fluxes derived from measured activities should be applicable to directly calculated fluxes. A nominal value of ±25% was selected from Table 4-1 for determination of average flux in surveillance capsules. Uncertainty limits associated with spatial extrapolation from capsule to maximum location in the pressure vessel and to account for variation of relative power distribution between fuel cycles cause the overall uncertainty limit to increase to ±30% for predicted fluence over the pressure vessel life (Table 4-2). Power distribution effects are estimated to be predictable within ±20% with a method based on comparison of total fast flux escaping the reactor core (section 2.3.5). It should be emphasized that this ±30% value is dependent on the availability of a core criticality analysis for an equilibrium fuel cycle and that this fuel cycle be utilized over most of the vessel life. Also, the uncertainty limits of a considerable number of the components included in the overall value have been estimated due to the absence of specific data. The net effect is to diminish the credibility of the overall uncertainty limits listed in Table 4-2. However, an attempt was made to select conservative values (maximum expected variations) for each identifiable component.

Because operating procedures, fuel enrichments, etc., vary between 177-FA reactors, the power distribution from a specific fuel cycle does not correspond

to that in a generic analysis. Selection of average cycle power distributions will introduce an additional uncertainty. In general, however, a cycle representing maximum fluence conditions (maximum fast flux escaping the reactor core) is used so that any extension of the uncertainty limit is on the negative side (and usually ignored).

Table 4-1. Uncertainties Related to Dosimeter Analyses, %

	Reaction			
	$^{237}Np(n,f)$	$^{238}U(n,f)$	$^{54}Fe(n,p)$	$^{58}Ni(n,p)$
Measured dosimeter activity[18]	±21	±13	±13	±13
Calculated dosimeter activity[a]	±34	±29	±29	±29
Conversion of activity to flux	±11(±21)[b]	±11	±11	±11
Flux (based on measured activity)	±20(±30)[b]	±17	±17	±17
Fast flux (E > 1 MeV)	±24(±30)[b]	±17	±26	±26

[a] An additional component was added to the reference 18 uncertainty analysis to account for relative power distribution averaging over the irradiation period.

[b] Values in parenthesis are based on the yield data used in the initial surveillance capsule analyses. Updated yield data will produce lower values (Table D-2).

Table 4-2. Uncertainty Limits Associated With Generic Pressure Vessel Surveillance Flux Analysis for 177-FA Reactors

	Uncertainty, %[a]
Fast flux based on capsule dosimeter measurements	±21[b]
Maximum fast flux in pressure vessel region	±23
Pressure vessel fluence prediction over 32-year vessel life	±30[c]

(a) Values associated with fast flux are considered applicable to fluence because reactor operating power measurements (and their duration) measurements are relatively accurate.

(b) Nominal value from all dosimeter reactions.

(c) Based on a reference fuel cycle.

5. RESULTS

5.1. Generic Design Fluence

A generic design curve was constructed so that the maximum fluence that will occur in the pressure vessel of any 177-FA reactor based on present B&W design parameters could be predicted. Calculated flux (benchmarked to capsule dosimetry) at the pressure vessel inside surface (~11° off a major axis) for Oconee 2, cycle 1, was used as a reference value and then adjusted to account for generic model conditions as follows:

$$\text{Fluence (generic)} = \left[\text{Calculated flux } (E > 1 \text{ MeV}) \text{ at inside surface of pressure vessel for Oconee 2, cycle 1}\right] \times \left[\text{Ratio of generic power to Oconee 2 power}\right] \times \left[\text{Ratio of cycle-averaged core escape flux over extreme equilibrium cycle to Oconee 2, cycle 1}\right] \times \left[\text{Upper uncertainty limit of predicted equilibrium cycle conditions}\right] \times \left[\text{Pressure vessel design life in seconds}\right]$$

The terms of this equation are based on the following conditions. A generic power rating of 2772 MWt represents the maximum power presently considered for B&W 177-FA reactors. For a given relative power distribution, flux escaping the core should be directly proportional to power level. Change in relative power distribution is accounted for by the ratio of fast flux escaping the core. This direct proportionality to pressure vessel fluence is based on the premise that all 177-FA reactors have the same flux attenuation characteristics from core edge to pressure vessel (section 2.3.5). A review of available core calculations performed for fuel management analyses indicated that ANO-1, cycle 3, should represent the equilibrium cycle expected to have the greatest flux per unit power escaping the core (and therefore greatest pressure vessel fluence per unit power). To ensure that the generic curve

represents the extreme case, the upper uncertainty limit of 10% assigned to predicted power distributions is included. Thus,

$$\text{Fluence} = (1.39 \times 10^{19}) \left(\frac{2772}{2568}\right) \left(\frac{6.20 \times 10^{13}}{4.82 \times 10^{13}}\right) (1.1) (1.01 \times 10^{9})$$

$$= 2.1 \times 10^{19} \ \text{n/cm}^2.$$

Fluence as a function of operating time is plotted in Figure 5-1, with the inclusion of a ±30% uncertainty limit (Table 4-2). A fluence of 2.1×10^{9} n/cm^2 ±30%, which corresponds to 32 EFPY of reactor operation, is predicted to occur at the maximum location on the pressure vessel and under the most adverse conditions anticipated for 177-FA reactor. Possible changes in fuel management procedures, such as the use of an 18-month LBP fuel cycle, under consideration by several utilities, could result in fluence reductions of up to 25%.

Additional confidence in these data was obtained from the analytical procedure developed in section 4.2. A direct calculation of pressure vessel fluence based on ANO-1, cycle 3 power distributions and the calculational normalization factor from cycle 1 capsule data (section 3.2.3) yielded an end-of-life fluence of 2.1×10^{19} n/cm^2.

5.2. Specific Reactor Fluence

Fluence data derived from dosimeters in specific reactors have been extrapolated by use of a technique described in sections 2.3.5 and 4.2. The last cycle for which core escape fluxes were available was considered to be the equilibrium cycle, which was then assumed to be repeated to 32 EFPY (pressure vessel design life). These data indicate that a somewhat lower fluence will be reached at end-of-life than predicted by the generic curve (Table 5-1). This difference is accounted for by the higher power level and extreme cycle conditions utilized in the generic analysis. A ±30 uncertainty limit should also apply to specific plant extrapolated data. Note that the ANO-1 fluence of 1.3×10^{19} n/cm^2 is considerably lower than all other systems, primarily because of Arkansas Power & Light's decision to use the 18-month, LBP fuel cycle starting with the fourth cycle. Fluence levels for each pressure vessel weld considered to be in the beltline region can be determined from data listed in Appendix F for Oconee 1, 2, and 3, Three Mile Island 1 and 2, Crystal River 3, Rancho Seco, and ANO-1.

As surveillance capsule dosimetry data become available from future reactor operation, it will be used if necessary to refine the generic curve. Long term irradiation data will reduce the required extrapolation period (out to 32 EFPY) and provide a better indication of equilibrium cycle power distributions, which should tend to reduce the present uncertainty limit. Also, as data from multiple fuel cycle irradiation periods are obtained, a better definition of extreme cycle conditions could permit an additional reduction in generic fluence.

5.3. Lead Factors

A convenient method for translating fast flux values presented in this report (inside surface of pressure vessel) to other locations is by use of a lead factor. Lead factor is defined as the ratio of fast flux at a specific location to the maximum fast flux in the pressure vessel. In this analysis maximum flux occurs at the inside surface of the pressure vessel on a radial traverse located ~11° off a major axis (Rθ geometric model). Values for pertinent locations are listed in Table 5-2. These ratios were determined from a radial flux distribution obtained from a one-dimensional radial ANISN calculation. Although the calculational model was based on major axis dimensions, the lead factors should be applicable to any radial traverse (in this case 11° off axis) because flux distribution near the pressure vessel is primarily a function of attenuation in the radial direction due to symmetry in planar geometry of nearby regions (Figure 2-1).

Lead factors for different azimuthal locations (points not on the same radial traverse) are somewhat sensitive to variations that occur in azimuthal flux distribution between reactors; as contrasted to the shape of radial flux distributions which is relatively consistent for 177-FA reactors in regions near the pressure vessel. In general, however, maximum and minimum azimuthal values were located at about 11° and 26°, respectively. The corresponding azimuthal displacement factor in Table 5-2 represents the assumed equilibrium cycle (ANO-1, cycle 3). Since cycle averaged flux and fluence are directly proportional, these lead factors are also applicable to fluence. Thus, any fluence value from Figure 2-5 or Table 5-1 can be converted to a different location by multiplication with a lead factor.

Table 5-1. Maximum Pressure Vessel Fluence Prediction for 177-FA Reactors

Reactor	Power, MWt	Fast fluence, n/cm^2			
		Based on capsule irradiation	Extrapolation to equilibrium cycle[a]	Extrapolation to 32 EFPY	Uncertainty limit
Oconee 1	2568	8.9(+17)	1.8(+18)	1.7(+19)	±30%
Oconee 2	2568	5.3(+17)	1.9(+18)	1.8(+19)	±30%
Oconee 3	2568	4.2(+17)	1.5(+18)	1.9(+19)	±30%
TMI-1	2535	5.7(+17)	1.8(+18)	1.7(+19)	±30%
ANO-1	2568	4.1(+17)	2.6(+18)	1.3(+19)	±30%
Generic	2772	--	--	2.1(+19)	±30%

(a) Equilibrium cycle assumed to be the last cycle (≥ 3) for which fuel management analysis data (core escape fluxes) are available.

Table 5-2. Lead Factors for Fast Flux in a 177-FA Reactor

Location		Radial displacement factor	Azimuthal displacement factor	Lead factor
Radial	Azimuthal[a]			
Capsule center	11°	1.8	1.0	1.8
Vessel inside surface	11°	1.0	1.0	1.0
T/4[b]	11°	1/1.8	1.0	1/1.8
3 T/4	11°	1/7.5	1.0	1/7.5
Vessel outer surfaces	11°	1/17.5	1.0	1/17.5
Capsule center	26°	1.8	1/1.4	1.3
New capsule center[c]	11°	4.5	1.0	4.5
New capsule center[c]	26°	4.5	1/1.4	3.2

[a] Location of maximum (11°) and minimum (26°) of azimuthal flux variation based on ANO-1, cycle 3 power distribution.

[b] T = thickness of pressure vessel.

[c] Capsule location in the three host reactors — Three Mile Island 2, Crystal River 3, and Davis-Besse 1.

Figure 5-1. Generic Design Fluence for 177-FA Reactors Based on Location of Maximum Exposure on Inside Surface of Pressure Vessel

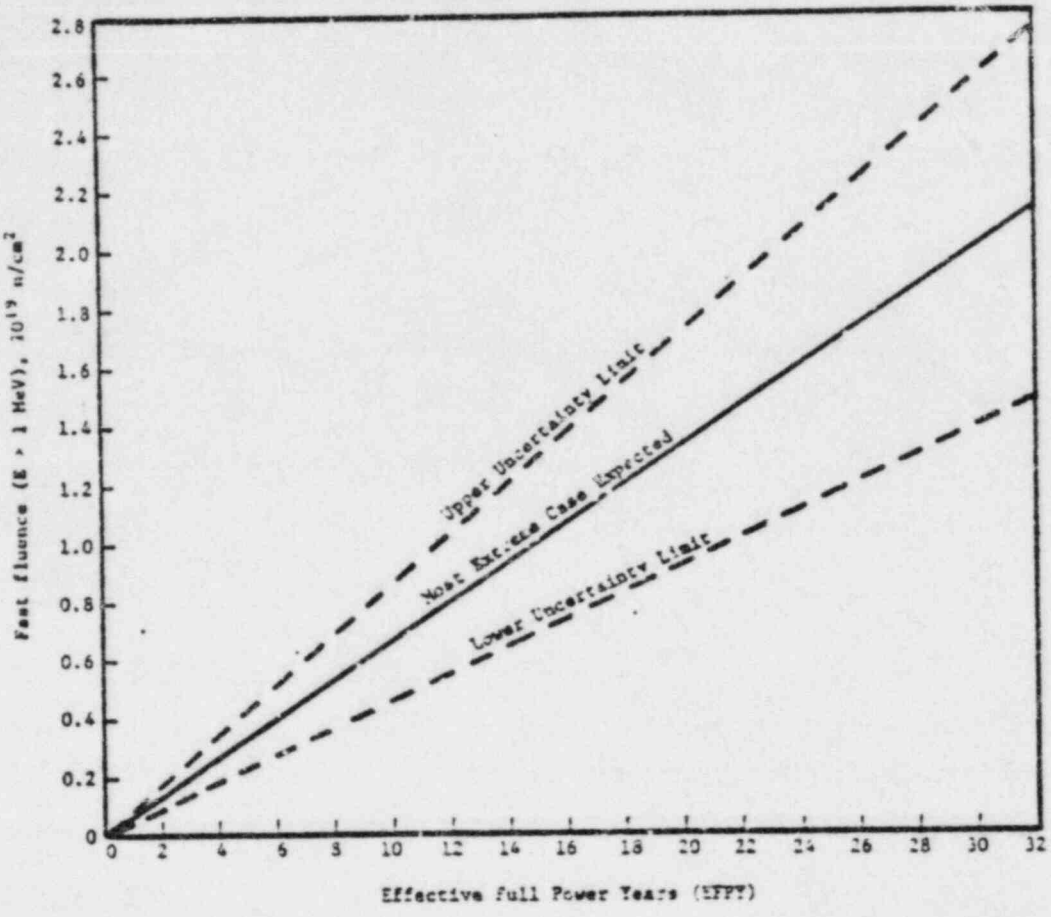

6. REFERENCES

1. Code of Federal Regulations, Chapter 10, Part 50, Appendix G, "Fracture Toughness Requirements."

2. Code of Federal Regulations, Chapter 10, Part 50, Appendix H, "Reactor Vessel Materials Surveillance Program Requirements."

3. Reactor Vessel Material Surveillance Program, BAW-10006, Rev 1, Babcock & Wilcox, Lynchburg, Virginia, May 1970.

4. H. S. Palme, G. S. Carter, and C. L. Whitmarsh, Reactor Vessel Material Surveillance Program — Compliance With 10CFR50, Appendix H, for Oconee Class Reactors, BAW-10100A, Babcock & Wilcox, Lynchburg, Virginia, February 1975.

5. J. J. Sapyta, K. M. Newlon and N. M. Hassan, User's Manual for B&W's Version of ANISN, NPGD-TM-128, Babcock & Wilcox, Lynchburg, Virginia, December 1971.

6. User's Manual for the DOT-IIW Discrete Ordinates Transport Computer Code, WANL-TME-1982, December 1969.

7. CASK — 40-Group Coupled Neutron and Gamma Ray Cross Section Data, RSIC-DLC-23, Radiation Shielding Information Center, Oak Ridge, Tennessee.

8. H. A. Hassan, et al., Power Peaking Nuclear Reliability Factors, BAW-10119P, Babcock & Wilcox, Lynchburg, Virginia, June 1977.

9. W. M. Herwig and N. M. Hassan, SORREL — DOT Input Generation Code, NPGD-TM-427, Babcock & Wilcox, Lynchburg, Virginia, November 1977.

10. W. T. Brunson to L. B. Wimmer, Memorandum, "Axial Power Shapes for Gamma Heating Analysis," 12511.9, Babcock & Wilcox, February 22, 1973.

11. A. L. Lowe, Jr., et al., Analysis of Capsule OCI-F From Duke Power Company, Oconee, Unit 1 — Reactor Vessel Materials Surveillance Program, Revision 1, BAW-1421, Rev. 1, Babcock & Wilcox, Lynchburg, Virginia, September 1975.

12 A. L. Lowe, Jr., et al., Analysis of Capsule OCI-E, Duke Power Company Oconee Nuclear Station, Unit 1 — Reactor Vessel Materials Surveillance Program, BAW-1436, Babcock & Wilcox, Lynchburg, Virginia, September 1977.

13 A. L. Lowe, Jr., et al., "Analysis of Capsule OCII-C From Duke Power Company Oconee Nuclear Station, Unit 2 — Reactor Vessel Materials Surveillance Program, BAW-1437, Babcock & Wilcox, Lynchburg, Virginia, May 1977.

14 A. L. Lowe, Jr., et al., Analysis of Capsule OCIII-A From Duke Power Company Oconee Nuclear Station, Unit 3 — Reactor Vessel Materials Surveillance Program, BAW-1438, Babcock & Wilcox, Lynchburg, Virginia, July 1977.

15 A. L. Lowe, Jr., et al., Analysis of Capsule TMI-1E From Metropolitan Edison Company Three Mile Island Nuclear Station, Unit 1 — Reactor Vessel Materials Surveillance Program, BAW-1439, Babcock & Wilcox, Lynchburg, Virginia, January 1977.

16 A. L. Lowe, Jr., et al., "Analysis of Capsule ANI-E From Arkansas Power & Light Company, Arkansas Nuclear One, Unit 1 — Reactor Vessel Materials Surveillance Program, BAW-1440, Babcock & Wilcox, Lynchburg, Virginia, April 1977.

17 R. G. Helmer and R. C. Greenwood, "Evaluated Decay Scheme Data," Nuclear Technology 25 (1975), pp 258-273.

18 L. A. Hassler, Reactor Vessel Surveillance Program Uncertainty Report (to be published).

19 M. E. Meek and B. F. Rider, "Compilation of Fission Product Yields," NEDO-12154-1, Vallecitos Nuclear Center, General Electric Company, January 26, 1974.

20 W. N. McElroy and L. S. Kellogg, "Fuels and Materials Fast-Reactor Dosimetry Data Development and Testing," Nuclear Technology 25 (1975), pp 180-223.

APPENDIX A

Time Averaging of Relative Power Distributions

To provide a single RPD that will represent an entire irradiation period the following calculation method is used. It is based on the assumption that the values vary linearly with burnup except when control rod movement occurs, and then a step change occurs. For example, let q_0, q_{50}, q_{100}, q_{150}, q_{200}, and q_{250}, represent the relative power at a specific location at 0, 50, 100, 150, 200 and 250 days during a 250-day fuel cycle. At 200 days control rods are moved. Thus,

$$\bar{q} = \frac{1}{250}\left[25q_0 + 50q_{50} + 50q_{100} + 75q_{150} + 25q_{200} + 25q_{250}\right]$$

This averaging calculation is performed by the code SORREL. Effectively, this formulation indicates that q_0 applies from 0 to 25 days, q_{50} from 25 to 75 days, q_{100} from 75 to 125 days, q_{150} from 125 to 200 days, q_{200} from 200 to 225 days, and q_{250} from 225 to 250 days.

APPENDIX B

Axial Power Distribution Correction Factors

For a given fuel assembly, end-of-cycle burnups as a function of axial location are obtained from fuel management analyses. Relative power distribution is obtained by dividing local burnup by the average burnup for that fuel assembly. From this distribution, peak (or correction) factors are calculated for the surveillance capsule elevation and for the maximum axial location. (Although, in principle, factors for any axial location could be calculated). These factors are then weighted to account for fuel assembly location. From Figure 2-1 it can be seen that values from the H, K, and L rows should be representative of the flux escaping the core that reaches the capsule located at 11° off axis.

Weighting factors were calculated to account for exponential attenuation of fast neutrons born in interior fuel assemblies. Thus,

Column	Attenuation distance, cm	Weighting factor
15	0.0	1.0
14	21.8	$e^{-\Sigma_R T} = e^{-(0.07)(21.8)} = 0.22$
13	43.6	$e^{-\Sigma_R T} = e^{-(0.07)(43.6)} = 0.05$

where $\Sigma_R = 0.07\ cm^{-1}$ is the macroscopic removal cross section calculated in the core region for neutrons and has been averaged over the energy range $E > 1$ MeV and weighted with a fission spectrum. All neutrons born in a fuel assembly are assumed to be located at the outer edge so that the attenuation distance is a multiple of a fuel assembly pitch. The rapid reduction of this factor indicates that only the outer two assemblies significantly contribute to flux escaping the core.

The axial power distribution factor, F_z, can be calculated for each row as follows:

$$F_{ZH} = \frac{1}{1.27}\left[\left(\frac{q}{\bar{q}_{H15}}\right) + 0.22\left(\frac{q}{\bar{q}_{H14}}\right) + 0.05\left(\frac{q}{\bar{q}_{H13}}\right)\right]$$

where $(q/\bar{q}_{H15})$ is the relative power density in assembly H15, etc.

Values of q'/q should be near the same elevation for each assembly. A core average value is obtained by giving equal weight to the values of H, K, and L. Admittedly this is an approximate procedure but RPD values do not vary significantly from pin to pin as shown in the following example from Oconee 3, cycle 1 data (Table B-1).

The use of axial factors to correct RE flux calculations at locations outside the core is predicated on the assumption that axial flux shape in the core is the same as the axial power shape and that this shape remains intact outside the core. For these reactor problems, this appears to be a reasonable assumption because of the regular geometry of the attenuation regions (structural components) at the elevation of interest (core height). In practice, (calculations in RZ geometry of similar reactor models) the axial shape has been observed to flatten somewhat at increasing distance from the core. This would tend to make flux predictions with these axial factors slightly high.

Table B-1. Determination of a Typical Axial Correction Factor

Fuel assembly	Weighting factor	F_z	
		Average over surveillance capsule length	Peak axial location
H15	1.0	1.17	1.13
H14	0.22	1.16	1.17
H13	0.05	1.18	1.17
H Row	—	1.17	1.18
K15	1.0	1.17	1.18
K14	0.22	1.16	1.17
K13	0.05	1.18	1.17
K Row	—	1.17	1.18
L15	1.0	1.16	1.17
L14	0.22	1.13	1.13
L13	0.05	1.10	1.10
L Row	—	1.16	1.16
Core average	—	1.17	1.18

BLANK FRAME

FOR

PROPER PAGINATION

APPENDIX C

Effective Energy Range for Dosimeter Reactions

In order to properly evaluate the flux data derived from dosimeter reactions, the energy range over which those reactions occur must be known. This effective energy is defined as that energy above which ~95% of the reactions occur and is a function of the flux spectrum. Values were calculated using fission spectrum-averaged microscopic capture cross sections and the relative flux spectrum at the dosimeter location. Reaction rate data were calculated for the flux spectrum that existed at the capsule location from the reference model calculation. These data, itemized in Table C-1, indicate effective energy ranges of >0.5 MeV for $^{237}Np(n,f)$, >1.0 MeV for $^{238}U(n,f)$, >2.3 MeV for $^{58}Ni(n,p)$, and >2.5 MeV for $^{54}Fe(n,p)$ reactions. These energies are somewhat dependent on the group structure used in the flux spectrum calculations and, therefore, should not be considered absolute values. However, they are consistent with other neutron transport calculations performed in the surveillance capsule analyses.

Table C-1. Effective Energy Range for Dosimeter Reactions

Energy group	Lower energy bound, MeV	Normalized flux	Cumulative reaction rate			
			$^{237}Np(n,f)$	$^{238}U(n,f)$	$^{58}Ni(n,p)$	$^{54}Fe(n,p)$
1	12.2	7.0(-4)	1.74(-3)	3.56(-3)	3.74(-3)	4.22(-3)
2	10	2.85(-3)	8.87(-3)	1.69(-2)	2.43(-2)	2.59(-2)
3	8.18	8.19(-3)	3.09(-2)	5.54(-2)	8.69(-2)	9.36(-2)
4	6.36	2.24(-2)	8.19(-2)	1.53(-1)	2.53(-1)	2.82(-1)
5	4.96	4.11(-2)	1.50(-1)	2.70(-1)	5.11(-1)	5.58(-1)
6	4.06	3.50(-2)	2.07(-1)	3.63(-1)	6.75(-1)	7.19(-1)
7	3.01	5.25(-2)	3.04(-1)	5.01(-1)	8.36(-1)	8.72(-1)
8	2.46	5.43(-2)	4.02(-1)	6.43(-1)	9.24(-1)	9.46(-1)
9	2.35	1.75(-2)	4.34(-1)	6.89(-1)	9.42(-1)	--
10	1.83	6.78(-2)	5.57(-1)	8.61(-1)	--	--
11	1.11	1.24(-1)	7.68(-1)	9.96(-1)	--	--
12	5.5(-1)[a]	1.36(-1)	9.45(-1)	--	--	--
13	1.1(-1)	1.94(-1)	--	--	--	--
14	3.35(-3)	2.44(-1)	--	--	--	--

[a] Read as 5.5×10^{-1}

BLANK FRAME

FOR

PROPER PAGINATION

APPENDIX D

Weighted Capture Cross Sections and Fission Yields

Microscopic capture cross sections for the dosimeter reactions of interest, and over the energy group structure used for transport calculations (Table 2-3), were obtained by weighting ENDF/BIV data over a fission spectrum. Consequently

$$\sigma = \frac{\int_{E_L}^{E_u} \sigma(E)\phi(E)dE}{\int_{E_L}^{E_u} \phi(E)dE}$$

for each energy group. The resulting data are listed in Table D-1.

Fission yields used to convert calculated flux to activity are itemized in Table D-2. Data from reference 19, used in the capsule analyses, were considered the best compilation at that time. However, updated values from reference 20 will be used in future analyses. Note that a significant increase will occur in calculated ^{137}Np fission product activities. This would improve experimental data comparisons presented in section 3.3.

Table D-1. Fission Spectrum Weighted Capture Cross Sections for Dosimeter Materials

Group	Lower energy bound, MeV	Weighted microscopic cross section, barns/atom			
		$^{237}Np(n,f)$	$^{238}U(n,f)$	$^{58}Ni(n,p)$	$^{54}Fe(n,p)$
1	12.2	2.321	1.073	0.4598	0.425
2	10	2.340	0.981	0.622	0.537
3	8.18	2.308	0.991	0.659	0.583
4	6.36	2.09	0.9165	0.638	0.572
5	4.96	1.54	0.600	0.540	0.473
6	4.06	1.533	0.562	0.403	0.325
7	3.01	1.616	0.553	0.264	0.206
8	2.46	1.691	0.550	0.139	0.096
9	2.35	1.695	0.553	0.089	0.0524
10	1.83	1.676	0.535	0.051	0.022
11	1.11	1.593	0.229	0.0128	0.0115
12	5.5(-1)[a]	1.217	0.008	4.8(-4)	—
13	1.1(-1)	0.1946	1.3(-4)	—	—
14	3.35(-3)	0.0410	—	—	—

[a] Read as 5.5×10^{-1}.

Table D-2. Fission Yield

Fission product	Yield, %			
	$^{237}Np(n,f)$		$^{238}U(n,f)$	
	Ref. 19	Ref. 20	Ref. 19	Ref. 20
^{137}Cs	~~6.38~~ 6.44	6.67	6.28	6.194
^{95}Zr	~~5.27~~ 5.51	5.85	5.30	5.324
^{103}Ru	~~4.67~~ 5.32	5.75	6.35	6.336

BLANK FRAME

FOR

PROPER PAGINATION

APPENDIX E

Equivalence of Activity and Flux Ratios

Activity of a dosimeter used to measure fluence can be obtained from

$$D = K \times FI \times PI \quad \mu Ci/g \text{ of target material}$$

where

$$K = \frac{f(6.023 \times 10^{23})}{M(3.7 \times 10^{4})},$$

FI = flux integral

$$= \int_E \sigma(E)\phi(E),$$

PI = power integral

$$= \sum_j F_j(1 - e^{-\lambda_i t_j})e^{-\lambda_i(T-\tau_j)}.$$

(see section 3.2.2 for term definitions).

K is a constant for a given reaction

$$\frac{D_{meas}}{D_{calc}} = \frac{FI_{meas} \times PI_{meas}}{FI_{calc} \times PI_{calc}}$$

And, if the power integral has been calculated correctly, $PI_{meas} = PI_{calc}$. It should be noted that for long-lived isotopes, this term is relatively insensitive to errors in power history and is primarily dependent on total irradiation time which is generally easy to determine. Thus,

$$\frac{D_{meas}}{D_{calc}} = \frac{FI_{meas}}{FI_{calc}} = \frac{\int_j \sigma(E)\phi(E)}{\int_E \sigma(E)\phi(E)}$$

For a given spectral distribution

$$\int_E \sigma(E)\phi(E) = \bar{\sigma}\Phi$$

where $\bar{\sigma}$ = average cross section over the energy range of interest,

Φ = flux integrated over the energy range.

If the calculated flux spectrum is identical to the actual spectrum, then the averaged cross sections will be equal.

$$\bar{\gamma}_{meas} = \bar{\gamma}_{calc}$$

and it follows that

$$\frac{D_{meas}}{D_{calc}} = \frac{\bar{\gamma}_{meas} \times \rho_{meas}}{\bar{\gamma}_{calc} \times \rho_{calc}} = \frac{\phi_{meas}}{\phi_{calc}}$$

BLANK FRAME

FOR

PROPER PAGINATION

APPENDIX F

Design Fluence for Beltline Region Welds

Determination of fluence for a specific location in the pressure vessel of a reactor requires knowledge of flux distribution in three dimensions, i.e., both Rθ and RZ model calculations. Such an effort for equilibrium cycle conditions for each reactor would probably be both excessive and impractical. Not only would the analytical effort require considerable manhours and computer hours, but equilibrium cycle conditions as presently conceived will probably be changed in the future. Therefore, specific reactor weld fluences have been based on the generic design curve (Figure 5-1) which should exceed expected values in most reactors. If problems result, data for specific reactors can be recalculated with specific reactor power distributions.

In Table F-1, factors are presented to convert the maximum fluence presented in Figure 5-1 to account for spatial location and power level for beltline region welds in each reactor. A specific fluence can be obtained from

$$\text{Weld fluence} = \left[\begin{matrix}\text{Fluence} \\ \text{from} \\ \text{Fig. 5-1}\end{matrix}\right] \times F_P \times F_\theta \times F_A \times F_R$$

where

F_P = power factor

$$= \frac{\text{specific reactor power in MW}}{2772},$$

F_θ = azimuthal spatial factor

$$= \frac{\text{flux at specific azimuthal location}}{\text{flux along 11° off axis radius}},$$

F_A = axial spatial factor

$$= \frac{\text{flux at specific axial location}}{\text{flux at maximum axial location}},$$

F_R = radial spatial factor (lead factor)

$$= \frac{\text{flux at specific radial location}}{\text{flux at inside surface of pressure vessel}}.$$

Relative factors for azimuthal and axial locations were obtained from analytical models that utilized equilibrium cycle power distributions. Weld fluence values calculated from Figure 5-1 and Table F-1 will have an estimated uncertainty of ±50%, although the conservative procedures used should bias the results on the high side.

Table F-1. Design Fluence Factors for Beltline Region Welds in 177-FA Reactors

Reactor	Welds: Location	Welds: Number	Power factor, F_2	Spatial factors: Azimuthal, F_ϕ	Spatial factors: Axial, F_z	Spatial factors: Radial, $F_{z\phi}$
Oconee 1	Outlet nozzle	(a)	0.93	1.0	5.4(-3)[c]	1.0
	Nozzle belt to intermediate shell	SA 1135	0.93	1.0	3.16	1.0
	Intermediate to upper shell	SA 1229, 61% ID[b] WF 25, 39% OD[b]	0.93	1.0	3.76	1.0
	Upper shell to lower shell	SA 1385	0.93	1.0	1.0	1.0
	Lower shell to dutchman	(a)	0.93	1.0	5.6(-3)	1.0
	Intermediate shell, longitudinal	SA 1073 (both seams)	0.93	0.79	1.0	1.0
	Upper shell, longitudinal	SA 1493 (both seams)	0.93	0.73	1.0	1.0
	Lower shell, longitudinal	SA 1430 (both seams)	0.93	0.69	1.0	1.0
Oconee 2	Outlet nozzle	(a)	.93	1.0	5.4(-3)	1.0
	Nozzle belt to upper shell	WF 154	0.93	1.0	3.76	1.0
	Upper shell to lower shell	WF 25	0.93	1.0	1.0	1.0
	Lower shell to dutchman	(a)	0.93	1.0	5.6(-3)	1.0
Oconee 3	Outlet nozzle	(a)	0.93	1.0	5.4(-3)	1.0
	Nozzle belt to upper shell	WF 200	0.93	1.0	3.76	1.0
	Upper shell to lower shell	WF 97, 75% ID WF 70, 25% OD	0.93	1.0	1.0	1.0
	Lower shell to dutchman	(a)	0.93	1.0	5.6(-3)	1.0
TMI-1	Outlet nozzle	(a)	0.92	1.0	5.4(-3)	1.0
	Nozzle belt to upper shell	WF 70	0.92	1.0	3.76	1.0
	Upper shell to lower shell	WF 25	0.92	1.0	1.0	1.0
	Lower shell to dutchman	(a)	0.92	1.0	5.6(-3)	1.0
	Upper shell, longitudinal	WF 8 (both seams)	0.92	1.0	1.0	1.0
	Lower shell, longitudinal	SA 1129, 100% SA 1520, 37% ID SA 1494, 63% OD	0.92	0.84	1.0	1.0
TMI-2	Outlet nozzle	(a)	1.0	1.0	5.4(-3)	1.0
	Nozzle belt to upper shell	WF 193, 38% ID WF 223, 62% OD	1.0	1.0	3.76	1.0
	Upper shell to lower shell	WF 199, 52% ID SA 1778, 46% OD WF 182-1, 2% OD	1.0	1.0	1.0	1.0
	Lower shell to dutchman	(a)	1.0	1.0	5.6(-3)	1.0
	Upper shell, longitudinal	SA 1174, 50% ID[d] SA 1413, 40% OD SA 1426, 100%[d]	1.0	0.77	1.0	1.0
	Lower shell, longitudinal	SA 1426, 100% SA 1493, 100%	1.0	0.69	1.0	1.0

Table F-1. (Cont'd.)

Reactor	Welds		Power factor, F_2	Spatial factors		
	Location	Number		Azimuthal, F_4	Axial, F_5	Radial, F_6 [e]
CR-3	Outlet nozzle	(a)	0.89	1.0	5.4(-3)	1.0
	Nozzle belt to upper shell	SA 1769, 40% ID WF 149, 60% OD	0.89	1.0	3.76	1.0
	Upper shell to lower shell	WF 70	0.89	1.0	1.0	1.0
	Lower shell to dutchman	(a)	0.89	1.0	5.6(-3)	1.0
	Upper shell, longitudinal	WF 18, 100% WF 9, 100%	0.89	0.94	1.0	1.0
	Lower shell, longitudinal	SA 1580 (both seams)	0.89	0.84	1.0	1.0
Rancho Seco	Outlet nozz...	(a)	1.0	1.0	5.4(-3)	1.0
	Nozzle belt to upper shell	WF 133	1.0	1.0	3.76	1.0
	Upper shell to lower shell	WF 154	1.0	1.0	1.0	1.0
	Lower shell to dutchman	(a)	1.0	1.0	5.6(-3)	1.0
	Upper shell, longitudinal	WF 29 (both seams)	1.0	0.89	1.0	1.0
	Lower shell, longitudinal	WF 70, 71% ID WF 29, 27% OD WF 29, 100%	1.0	0.99	1.0	1.0
ANO-1	Outlet nozzle	(a)	0.93	1.0	5.4(-3)	1.0
	Nozzle belt to upper shell	WF 182-1	0.93	1.0	3.76	1.0
	Upper shell to lower shell	WF 112	0.93	1.0	1.0	1.0
	Lower shell to dutchman	(a)	0.93	1.0	5.6(-3)	1.0
	Upper shell, longitudinal	WF 18 (both seams)	0.93	0.74	1.0	1.0
	Lower shell, longitudinal	WF 18 (both seams)	0.93	0.78	1.0	1.0

(a) No weld identification numbers are available.

(b) 61% ID represents 61% of the weld material measured from the inside diameter of the pressure vessel. 39% OD represents 39% of the weld material measured from the outside diameter of the pressure vessel.

(c) Read as 5.4×10^{-3}.

(d) Longitudinal weld seams are listed separately when the weld material differs between seams.

(e) Values are for inside diameter of pressure vessel (maximum radial effect on weld fluence). If other radial locations in the pressure vessel are of interest, F_6 values can be calculated by calculating the ratio of fast flux at the point of interest to fast flux at the pressure vessel inside diameter using Figure F-1.

Figure F-1. Fast Flux Attenuation Through Pressure Vessel Wall